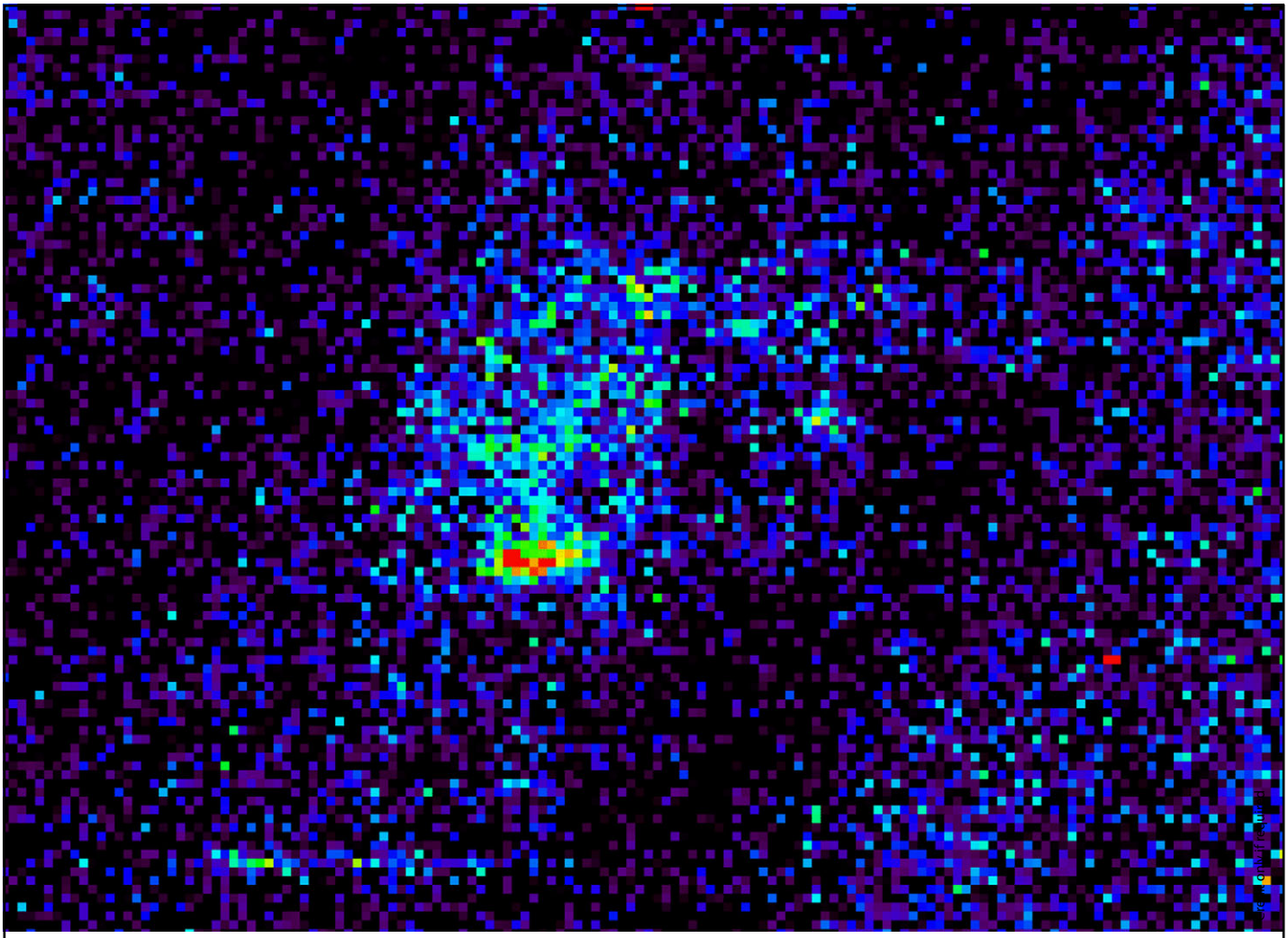

Showcasing research by Dr Lydia Finney into the role of metals and metalloproteins in biological systems at the X-ray Science Division, Advanced Photon Source, Argonne National Laboratory, Lemont, Illinois, USA

Identifying metalloproteins through X-ray fluorescence mapping and mass spectrometry

An approach to expose, identify and quantify metalloproteins in complex biological samples by sequential non-denaturing 2D-gel electrophoresis, X-ray fluorescence and tandem mass spectrometry. The method not only detects and distinguishes metals within the same spot of a sample but also characterizes the proteins that bind them.

Courtesy of Argonne National Laboratory, managed and operated by UChicago Argonne, LLC, for the U.S. Department of Energy under Contract No. DE-AC02-06CH11357.

As featured in:

See Lydia Finney *et al.*, *Metallomics*, 2012, **4**, 921–927

Metallomics

Dynamic Article Links
View Online

Cite this: *Metallomics*, 2012, **4**, 921–927

www.rsc.org/metallomics

PAPER

Identifying metalloproteins through X-ray fluorescence mapping and mass spectrometry†

Daniel Raimunda,[a] Tripti Khare,[b] Carol Giometti,[b] Stefan Vogt,[c] José M. Argüello[a] and Lydia Finney*[c]

Received 21st May 2012, Accepted 10th August 2012
DOI: 10.1039/c2mt20095c

Metals are critical and dynamic components of biochemistry. To understand their roles, we greatly need tools to identify the ligands that bind them within the complexity of natural systems. This work describes the development of methods that not only detect and distinguish metals, but also characterize the proteins that bind them. We describe an approach to expose, identify and quantify metalloproteins in complex mixtures by sequential non-denaturing 2D-gel electrophoresis (2D GE)/X-ray Fluorescence (XRF) and tandem mass spectrometry (MS/MS) in the same spot of a sample. We first apply the development of 2D GE/XRF to *Shewanella oneidensis* MR-1, a well-studied system, and verify our electrophoretic approach. Then, we identified a novel periplasmic zinc protein in *Pseudomonas aeruginosa* PAO1 through 2D GE/XRF followed by MS/MS. The identity and function of this protein was verified through a gene mutation experiment.

Introduction

Transition metals such as copper, zinc, or iron, are essential nutrients in all life kingdoms. They are also potentially toxic,[1] and are increasingly used in medicine as part of diagnostic reagents.[1b,2] As prosthetic groups of metalloproteins they perform much of the cellular chemistry critical to life.[3] Here, we describe an approach to detect, identify, and quantify metalloproteins from complex mixtures. Our studies focused on two microbial systems, *Shewanella oneidensis* MR-1 and *Pseudomonas aeruginosa* PA01. *Shewanella*, an environmental microbe, is a model organism for bacterial dissimilatory iron reduction which is dependent on multiple c-type cytochromes. *Pseudomonas* is a human pathogen and models the critical role metals play in infection.

Key metalloproteins in *Shewanella*

S. oneidensis MR-1 is a metal-reducing Gram-negative facultative anaerobe. It can utilize a broad spectrum of terminal electron acceptors including oxygen, nitrate, nitrite, fumarate, and, in the absence of oxygen, a wide variety of metals including iron, manganese, chromium, uranium.[4] *S. oneidensis* MR-1 has been shown to convert nitrate to ammonium and the soluble forms of U(VI) and Cr(VI) to the reduced, insoluble oxides U(IV) and Cr(III).[4] Thus, this microbe, along with other metal reducing bacteria such as species of *Geobacter* and *Desulfitobacterium*, has the capacity to remediate groundwater transport of uranium, chromium, and technetium and potentially block their leaching into rivers and potable groundwater supplies.[5]

The complete genome sequence of *S. oneidensis* MR-1 has revealed the complexity of its electron transport system, including 42 c-type cytochromes.[6] These iron-containing heme proteins play important roles in electron transport chains critical to anaerobic respiration and dissimilatory metal reduction pathways, as confirmed by gene mutation studies.[4,5] Many of these cytochromes are located in the outer membrane (OmcA and OmcB), or the plasma membrane (mtrA and mtrB). Importantly, the cytochrome content of *S. oneidensis* varies widely depending upon terminal electron acceptor availability.[7] Characterizing the *S. oneidensis* response to available electron acceptors through differential expression of its c-type cytochromes repertoire is crucial to fully understanding the electron transport mechanisms of this bacterium.

The struggle over metals in bacterial infection

In the case of bacterial infections, the struggle for micronutrients and against toxic metals determines the outcome of the host–pathogen interaction. On one side, in animals the activation of the innate immune system can led to reduction of the availability of essential transition metal nutrients.[8] The animal and plant hosts will also generate damaging reactive oxygen and nitrogen species, which mediate many of their toxic effects through interactions with metals and metalloproteins.

[a] *Department of Chemistry and Biochemistry, Gateway Park, Worcester Polytechnic Institute, 100 Institute Road, Worcester, MA 01609, USA*
[b] *Biosciences Division, Argonne National Laboratory, 9700 South Cass Avenue, Lemont, IL, USA*
[c] *X-ray Science Division, Advanced Photon Source, Argonne National Laboratory, 9700 South Cass Avenue, Lemont, IL, USA. E-mail: lfinney@aps.anl.gov; Tel: +1 630 252 0886*
† Electronic supplementary information (ESI) available. See DOI: 10.1039/c2mt20095c

On the other hand, microorganisms cope with this hostile microenvironment through catabolic enzymes such as alkylhydroperoxidase (AhpF) and peroxiredoxin (AhpC), by secreting antioxidant metalloenzymes like superoxide dismutase (SodA and SodC), and catalase (KatG) and by competing with the host for essential metal micronutrients. Consequently, the pathogen's proteins involved in the influx/efflux, storage and utilization of transition metal ($Fe^{2+/3+}$, $Cu^{+/2+}$, Zn^{2+}, Mn^{2+}, *etc.*) are likely to have a determinant role in pathogenesis. *P. aeruginosa* is an opportunistic human pathogen and infection with this organism can result in pneumonia or sepsis. The importance of metal homeostasis in its virulence has been shown.[9] Thus, it is critical to identify metalloproteins relevant to this process.

Gaining insights by combining proteomics and X-ray fluorescence

To better understand the biochemistry of metals in these systems, a critical need exists for technology that pairs information about metal occupancy with the identity of proteins in complex mixtures. The detection of metals in cells and bulk protein samples has become routine,[10] and has greatly aided our understanding of bioinorganic chemistry and the physiology of metalloproteins in the cell. However, to advance from understanding the chemistry of these proteins *in vitro*, to explaining their behavior *in vivo*, enabling methods to detect and quantify the metal component in single metalloproteins are necessary. This means monitoring dozens of metalloproteins in cell lysates and extracts, each binding specific metals, rather than analyzing purified individual proteins.

There are many on-going efforts towards this goal. Some utilize liquid chromatography for separation, others electrophoresis. Liquid chromatographic separations are particularly amenable to analysis by techniques such as ICP-MS, since the sample is kept in solution during the separation step.[11] Electrophoretic separations can also be analyzed by ICP-MS, typically requiring either physical extraction of spots, laser ablation (LA-ICP-MS)[12] or autoradiography.[13] Electrophoresis pairs remarkably well with synchrotron X-ray fluorescence (XRF) imaging,[14] which has advanced in recent years due to the development of third generation synchrotron sources, and zone plate focusing optics. Electrophoretically separated proteins can be transferred to blots and these are rigid and nearly transparent to X-rays at typical energies used to excite transition metals.[15] The powerful focused beams available at a synchrotron source such as the Advanced Photon Source provide the potential for sub-attogram per μm^2 sensitivity, with the simultaneous detection of over a dozen metals and the potential to perform X-ray absorption spectroscopy on the same samples.[16] But much room for growth and improvement remains, particularly in linking detected signal from metals to the identification of associated proteins.

We present here a direct and comprehensive approach to metalloproteomics that uses well-established, available techniques. This methodology separates and detects metalloproteins using non-denaturing 2D gel electrophoresis, with simultaneous quantitative detection of elemental content by XRF. This 2D gel analysis verified findings on the well-studied model system *S. oneidensis*. Applying these methods to *P. aeruginosa*, and adding MS/MS identification, we have found strong evidence to suggest that a predicted Fe-binding component of an ABC-transport system is in fact involved in zinc transport and homeostasis.

Experimental

Cell culture

S. oneidensis MR-1 was grown in minimal media consisting of 3 mM PIPES (piperazine-*N*,*N*′-bis(ethanesulfonic acid)), 7.5 mM NaOH, 30 mM NH_4Cl, 1.3 mM KCl, 4.5 mM NaH_2PO_4, pH 7.0, supplemented with 0.6% sodium lactate, 2 mg L^{-1} each of L-arginine, L-glutamic acid, and L-serine, and 10 mL L^{-1} of commercial vitamin and trace metal solutions MD-VS and MD-TMS (ATCC). In addition, aerobic cultures contained 30 mM NaCl and anaerobic cultures contained 100 mM sodium fumarate. Aerobic cultures were grown in 2 L baffled flasks containing 1 L of medium at 28 °C, 250 rpm, and were harvested at mid-log phase (0.5–1.0 OD_{600nm}). Anaerobic cultures were grown in 1 L screw capped bottles containing 1 L medium, purged with N_2 prior to inoculation and sealed with a sterile #6 rubber stopper. Cells were grown at 28 °C, 100 rpm, harvested at 0.15–0.30 OD_{600nm} and pellets stored at −80 °C.

P. aeruginosa PAO1 wild-type strain and PA5217 insertional mutant were obtained from the Comprehensive *P. aeruginosa* Transposon Mutant Library at the University of Washington Genome Center.[17] Cells were grown at 37 °C, 200 rpm in LB medium, supplemented with tetracycline (60 μg mL^{-1}) as required.

Shewanella oneidensis soluble-protein extract preparation

Frozen cells were thawed and immediately mixed with two volumes of lysis buffer containing 50 mM glucose, 25 mM Tris–HCl, pH 8.0, and 4 mg mL^{-1} lysozyme in the presence of protease inhibitors (Complete mini protease inhibitor cocktail; Roche Diagnostics, Indianapolis, IN, USA). Lysozyme was added to the lysis buffer immediately before use. Cells were lysed by three freeze–thaw cycles. Cell suspension was centrifuged for 30 min at 160 000 × *g*. Supernatant was collected and stored at −80 °C until further analysis. The total protein concentration of samples was determined using the Bio-Rad DC Protein assay system, which is similar to the well documented method of Lowry *et al.*[18]

Pseudomonas aeruginosa periplasmic-protein extract preparation

Cells were harvested at early stationary phase from 125 mL LB culture by centrifugation at 4000 × *g*, 4 °C for 10 min. The pellet was re-suspended and washed with ice-cold 30 mL of Tris–HCl 50 mM, pH 7.5, sorbitol 0.3 M (buffer S). Cells were recovered by centrifugation at 9000 × *g*, 4 °C for 10 min and washed again using the same buffer except that 10 μM ethylenediaminetetraacetic acid (EDTA)–Tris (pH 7.6) was included in the second wash and an incubation of 20 min at RT preceded centrifugation. A third wash was done in buffer S to remove remnant EDTA. Finally cells were re-suspended in ice-cold MilliQ H_2O, incubated for 5 min and centrifuged at 14 000 × *g*, 4 °C for 30 min. Supernatant was collected and

centrifuged again. The resulting supernatant was considered as the protein periplasmic fraction. Protein was concentrated using 3K-Centricon filter devices and stored at 5–10 mg mL^{-1} at −80 °C.

Non-denaturing 2D electrophoresis and electroblotting of protein samples

Prior to gel separations, all equipment was thoroughly rinsed with Milli-Q water. In the case of *Shewanella* samples, isoelectric focusing (IEF) was done using Invitrogen Zoom®IPGRunnerTM System. The immobilized pH gradient (IPG) strips of pH 5–7 were hydrated overnight with 155 μL of rehydration buffer containing 2% CHAPS, 0.2% Ampholyte (pH 3–10), 0.001% (w/v) bromophenol blue and 300 μg of protein sample. After overnight rehydration IEF was performed following the protocol B of step voltage as described in the system manual. After IEF, IPG strips were equilibrated in a pH 6.8 buffer containing 0.375 M Tris–HCl, 20% glycerol (v/v), and 0.001% (w/v) bromophenol blue, and then placed on top of 4–15% IPG-suited gels (Tris–Cl) from Bio-Rad. The second-dimension separation was done using the Laemmli buffer system without SDS.[19]

Use of the IPG step described for the *S. oneidensis* protein separation did not provide sufficient quantity of protein for the second-dimension gel for *Pseudomonas aeruginosa* periplasmic extracts, so the IEF was done using 1.5 mm polyacrylamide tubes (6 cm long) containing 5% (w/v) acrylamide, 3% (v/v) ampholytes pI range 3–10, 6% (v/v) ampholytes pI range 5–7 and 15% (v/v) glycerol. Protein samples (containing 50–100 μg protein) were added to an equal volume of sample buffer (1.3% (v/v) ampholytes pI range 3–10, 2.7% (v/v) ampholytes pI range 5–7, 76% (v/v) glycerol and 0.001% (w/v) bromophenol blue), loaded and focused at 500 V for 1 h. Second dimension electrophoresis was performed in 10% polyacrylamide gels. Denaturing (SDS, DTT, *etc.*) agents were not used in either electrophoresis. Total protein patterns were visualized in gels by using Coomassie Brilliant Blue for *Pseudomonas* samples.

For both *Shewanella* and *Pseudomonas* samples, duplicate, unfixed gels were blotted to PVDF membranes using a wet transfer system with Tris/glycine running buffer, for 1.5 h at 350 mA and 4 °C. Blots were then gently rinsed in Milli-Q H_2O, carefully dried free from dust, and stored covered in a petri dish prior to XRF.

X-ray fluorescence scanning of PVDF blots

PVDF blots were scanned in helium at beamline 8-BM-B of Sector 8, or at beamline 2-ID-E at the Advanced Photon Source (APS). Hard X-rays (10.2 keV) were monochromatized and passed through a pinhole (spot diameter on sample: 0.5 mm). Full X-ray fluorescence spectra were collected at each raster-scan step using a four element silicon drift detector (Vortex ME4, SII NanoTechnology). Spectra were fitted against NIST standards NBS1832 and NBS1833 or AXO standards (Blake Industries, Inc.) using per-pixel peak fitting algorithms with MAPS software.[20] This fitting creates maps of the gel specific for each element of the periodic table with atomic numbers ranging from sulfur ($Z = 16$) to zinc ($Z = 30$), with spatial resolution limited by the beam spot size, as well as the chosen sampling. Scanning of an entire PVDF blot (roughly 80 mm by 100 mm) typically took between 8–12 h depending on pixel resolution and dwell times.

Reduction, alkylation and tryptic digest for MS/MS

Images obtained by XRF were superimposed onto the PVDF membranes using fiduciary marks etched into the edges of the blot, and the spots corresponding to the metal signal were excised for tryptic digestion and LC-MS/MS identification. Briefly, PVDF membrane spots were transferred to 1.5 mL tubes and washed twice with 200 μL of 25 mM ammonium bicarbonate in 50% acetonitrile for 30 min at 37 °C. Spots were treated with 50 μL of 7.6 mg mL^{-1} DTT in 25 mM ammonium bicarbonate at 60 °C for 10 min. Subsequently, proteins in membrane spots were alkylated with 50 μL of 18.6 mg mL^{-1} iodoacetamide in 25 mM ammonium bicarbonate at room temperature for 1 h in the dark. The membranes were washed twice with 200 μL of 25 mM ammonium bicarbonate in 50% acetonitrile for 15 min at 37 °C and once with 50 μL acetonitrile for 10 min at room temperature. Samples were digested at 37 °C for 4 h, or overnight at 30 °C in 10 μL of 10 ng μL^{-1} trypsin and 40 μL of 25 mM ammonium bicarbonate, 20% acetonitrile. Soluble peptides were extracted and combined with the result of three washes of 50 μL of 50% acetonitrile, 5% formic acid (15 min). Extracted peptides were dried on a speed-vac and then dissolved in 20 μL 0.1% formic acid in water. Aliquots of tryptic peptides (2 μL) were first trapped on a hand-packed trap cartridge (100 μm × 2 cm Magic C18AQ 100 Å 5 μ C18) and then eluted and sprayed from a custom packed emitter (75 μm × 25 cm Magic C18AQ 100 Å 5 μ C18) with a linear gradient from 100% solvent A (0.1% formic acid in 5% acetonitrile) to 35% solvent B (0.1% formic acid in acetonitrile) in 90 min at a flow rate of 300 nl min^{-1} on a Proxeon Easy nanoLC system directly coupled to a Thermo LTQ Orbitrap Velos mass spectrometer. Data-dependent acquisitions were performed where full MS scans from 350–2000 Da were acquired in the Orbitrap at a resolution of 60 000 followed by 10 MS/MS scans on the most intense parent ions acquired in the LTQ ion trap instrument. The raw data file was searched against the proteobacteria subset of the Swissprot database using the Mascot Search engine (Matrixsciences, Ltd.). Parent mass tolerances were set to 15 ppm and fragment mass tolerances were set to 0.5 Da. The variable modifications of acetyl (protein *N*-term), pyro Glu for *N*-term Gln, propionamide of Cys and oxidation of Met were used. The output of the Mascot search result was loaded into Scaffold for in depth analysis of the identified proteins and peptides. MS/MS determinations were performed at the University of Massachusetts – Medical School, Proteomics and Mass Spectrometry Facility.

Results

Separation of samples from aerobically and anaerobically grown *Shewanella oneidensis* MR-1

Cell lysates from aerobically and anaerobically grown *S. oneidensis* MR-1 were subjected to 2D native electrophoresis

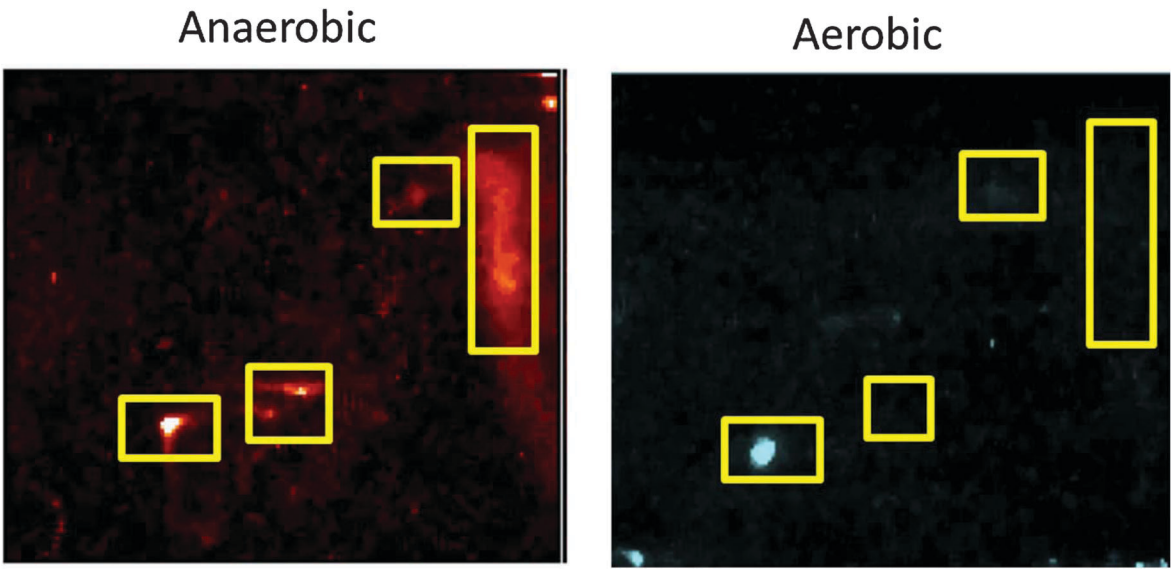

Fig. 1 Iron maps of *S. oneidensis* lysates. XRF imaging of these blots detected more iron-containing proteins in the anaerobic sample (left), as compared to the aerobic sample (right), as expected. Threshold values for these images are (in μg cm^{-2}): anaerobic, 609 max, 164 min; aerobic 459 max, 150 min.

and XRF (Fig. 1). The increase of iron-containing proteins was consistent with previous reports of the changes associated with switching from aerobic to anaerobic metabolism in this organism.[21]

The growth of *S. oneidensis* MR-1 under anaerobic conditions results in the increased expression of a number of specific iron-containing proteins (*e.g.*, fumarate reductase, superoxide dismutase-Fe, and c-type cytochromes) to such an extent that the cell pellets are visibly pink. Consequently, numerous iron proteins were observed by XRF imaging of blots of soluble proteins obtained from anaerobically grown *S. oneidensis* (Fig. 1). Producing predicted results in a well-characterized system, these images provide validation of the proposed methods.

While the *S. oneidensis* system is interesting, it is also complex. Over 121 genes are differentially expressed with the switch from aerobic to anaerobic respiration.[7a] For testing the pairing of 2D GE/XRF with MS/MS, we turned instead to the *P. aeruginosa*, where the process of interest associated with metal homeostasis takes place in the periplasmic compartment.[9]

Identification of proteins containing Zn by XRF-MS/MS in periplasmic fraction of *Pseudomonas aeruginosa* PAO1

As a Gram-negative bacterium, *P. aeruginosa* periplasm could perhaps be considered the 'front-line' of metal homeostasis. To study this compartment, periplasmic proteins obtained by cellular fractionation were resolved by 2D-electrophoresis. Resulting gels were stained with Coomassie brilliant blue (Fig. 2A) or proteins were transferred to PVDF membranes for XRF analysis. We relied on the signal from sulphur (Cys and Met residues) to evaluate the separation and transfer of proteins (Fig. 2B). Among several signals from a variety of transition metals (not shown) zinc spots were detected (Fig. 2C). The spots were excised from the membrane and analyzed by MS/MS. Results from three spots with low metal signal (green spots in Fig. 2C) yield no protein identification and probe inconsistent among sample replicates. However, the spot showing strong fluorescence signal (red spots in Fig. 2C) consistently yielded identifiable proteins. The MS/MS analysis showed the presence of two candidate zinc-containing proteins: PA5217 and PA0423 (Mascot score > 40) (spectra included as Fig. S1, ESI†). PA0423 has been characterized as an extracellular secreted protease involved in corneal erosion.[22] Its requirement of zinc for function has not been described. On the other hand, PA5217 is predicted to be the periplasmic component of an ABC transport system involved in Fe^{3+} import. Amino acid sequence of PA5217 shows high number of putative Zn^{2+} coordinating aminoacids (44 out of 333 aminoacids are D (17), E (20), H (5), C (2)). A protein blast search of PA5217 retrieves sequences from the periplasmic Fe^{3+} binding proteins of *Synecchocystis* PC6803, FutA1 and FutA2.[23] The crystallographic structures of both proteins were resolved in the holo form where Fe^{3+} is penta-coordinated by H54, Y55, Y185, Y241 and Y242 in FutA1, and by H44, Y45, Y169, Y230 and Y231 in FutA2.[24,25] All amino acids except H54/H44 are conserved in PA5217 and the identity/similarity values are 40/60% and 39/54% between PA5217 and FutA1 or PA5217 and FutA2, respectively. We have not found any example of a tetra-coordinate all-Tyr Zn^{2+} binding site, but Cys and His might present alternatives for Zn^{2+} coordination in PA5217. In addition, a survey of the genetic environment of the locus tag PA5217 indicates that this is part of a predicted operon containing also the membrane (PA52126) and cytoplasmic (PA5218) components required for a metal import ABC-ATPase. We have previously described bacterial ABC-transport systems with periplasmic components capable to bind and import Zn^{2+}.[26] The system is relevant for fitness and survival of bacteria *in vitro* under zinc starvation conditions. To functionally test Zn^{2+} binding to PA5217, a *P. aeruginosa* gene deletion mutant was obtained. As expected, the periplasmic fractions from the mutant strain showed sulphur signal similar in form and intensity to that of the wild

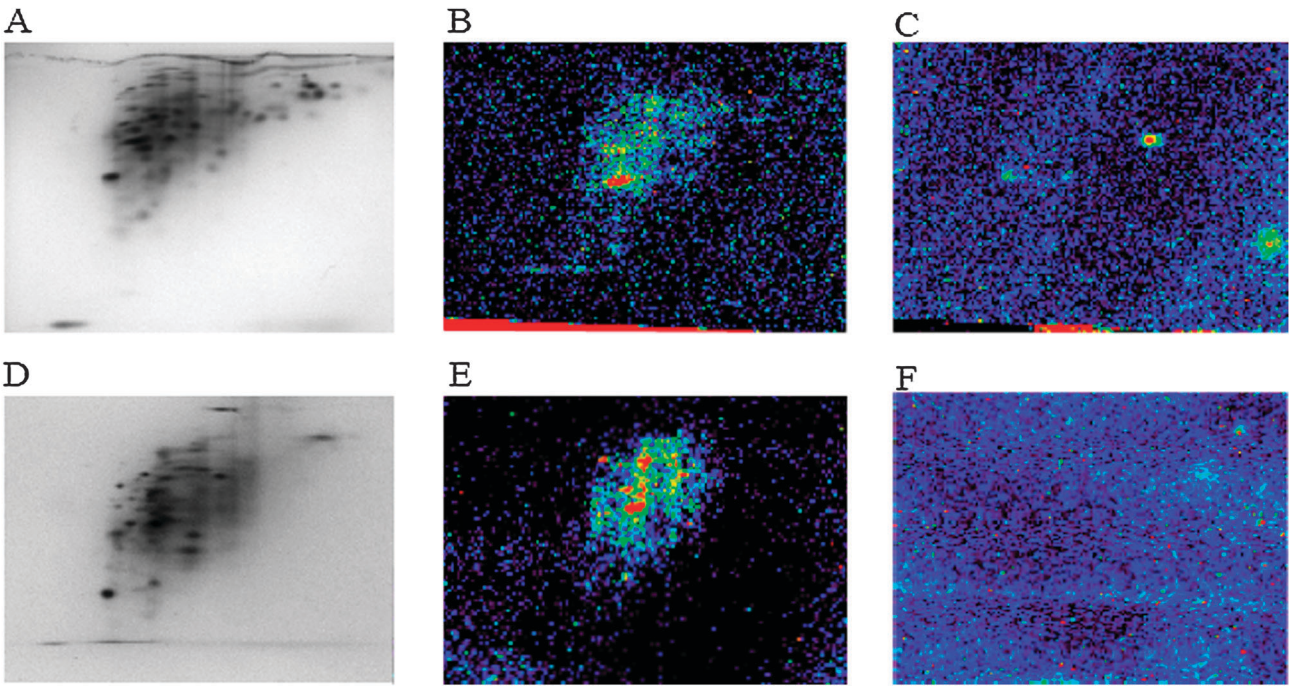

Fig. 2 2D GE/XRF images. Periplasmic protein fraction (100 μg) from *P. aeruginosa* PAO1 (A–C) and gene deletion mutant PA5217 (D–E) resolved by 2D-electrophoresis and (A, D) stained with Coomassie brilliant blue staining or (B, C, E, F) transferred to PVDF membrane and analysed by XRF, displaying sulphur (B, D) as a control for protein loading, and zinc (C, F). Data was fitted using MAPS.

type strain (Fig. 2E). However, it lacked the previously observed zinc containing protein (Fig. 2F).

The results obtained above suggest that protein PA5217 may be involved in Zn^{2+} homeostasis in *P. aeruginosa* functioning as periplasmic Zn^{2+}-binding component of the ABC-transport system. To test this role the PA5217 mutant strain was grown amending the culture media with EDTA, a divalent cation chelator. Mutant PA5217 showed an increased sensitivity to the presence of EDTA; *i.e.*, to metal starvation (Fig. 3).

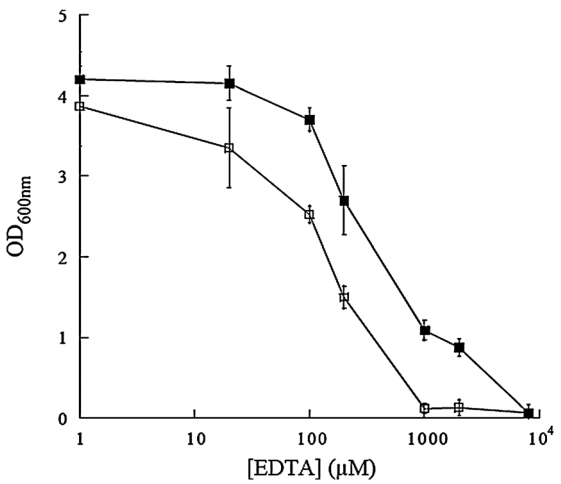

Fig. 3 *P. aeruginosa* growth under metal starvation. Cell growth under metal starvation condition. *P. aeruginosa* PAO1 (WT) (■) and deletion mutant PA5217 (□) cells were grown in LB supplemented with EDTA, for 16 h at 37 °C. Initial OD_{600nm} was 0.1, and OD_{600nm} values were measured after 16 h. Data represent the mean ± standard error (n = 3).

Additional experiments (Fig. S2, ESI†) showed that the PA5217 mutant cells grown in presence of EDTA were recovered by the addition of Zn^{2+} in the media (200 μM). Other metals (Fe^{3+}, Cu^{2+}, Ca^{2+}, Co^{2+} and Ni^{2+}) did elicit a much slower recovery than Zn, supporting the idea that PA5217 is part of an ABC Zn^{2+} import system. These conditions are also met by bacterial organisms during infections where the animal host innate immune response is to sequester micronutrients like Zn^{2+} and $Fe^{2/3+}$ [27] in the surroundings of the invaded tissue.[28]

Conclusions

We have developed methods for the native 2D GE separation of complex biological samples that are amenable with XRF analysis. As a proof of concept using commercially available metalloproteins, we previously showed the possibility of combining native 2D GE separations with XRF.[29] We now show the suitability of this approach for the analysis of complex biological samples. In addition, we have further extended this method to include MS/MS following the 2D native GE/XRF analysis. Consequently, this approach allows not only to determine changes in metal occupancy and/or metalloprotein pool sizes, but also to identify the associated protein. Moreover, the ultimate sensitivity of XRF detection is in the order of femto- to atto-grams per μm^2 of metal, and while this might be limiting to detect high turnover metal trafficking proteins or metalloproteins present in very low abundance, it represent a remarkable level of detection as showed in the described experiments.

On the other hand, we are cognizant of the limitations of the proposed methods. For instance, the intrinsic resolution of the

2D GE is likely to require the sorting among various proteins present in a single metal spot. Also, cell disruption and fractionation might alter the metal : protein complexes present *in vivo*. Yet, the required manipulation of samples is minimal compared with other approaches to protein separation (chromatography, ultra-centrifugation, *etc.*). Alternative metalloproteomic methods, such as autoradiography coupled with electrophoresis[13,30] and proteins separation/ICP-MS,[31,32] enable pulse-chase experiments to explore metalloproteins turnover kinetics. Finally, it should be emphasized that native 2D GE separation is accessible to most laboratories and resources for 2D XRF imaging are publicly available.

Acknowledgements

The use of the Advanced Photon Source was supported by the Department of Energy, Office of Science Contract DE-AC-02-06CH11357. This work was supported by NSF grant MCB-0743901 (JMA), and USDA-NIFA grant 2010-65108-20606 (JMA). The authors thank Evan Maxey for his assistance in optimizing the instrumentation for this work in its new home at 8-BM-B.

References

1 (*a*) L. A. Finney and T. V. O'Halloran, Transition metal speciation in the cell: Insights from the chemistry of metal ion receptors, *Science*, 2003, **300**, 931–936; (*b*) A. Levina and P. A. Lay, Chemical properties and toxicity of chromium(III) nutritional supplements, *Chem. Res. Toxicol*., 2008, **21**, 563–571; (*c*) A. Changela, K. Chen, Y. Xue, J. Holschen, C. E. Outten, T. V. O'Halloran and A. Mondragon, Molecular basis of metal-ion selectivity and zeptomolar sensitivity by CueR, *Science*, 2003, **301**, 1383–1387; (*d*) M. K. Jonsson, Q. D. Wang and B. Becker, Impedance-based detection of beating rhythm and proarrhythmic effects of compounds on stem cell-derived cardiomyocytes, *Assay Drug Dev. Technol*., 2011, **9**, 589–599.

2 (*a*) N. P. Chmel, L. E. Allan, J. M. Becker, G. J. Clarkson, S. S. Turner and P. Scott, TTF salts of optically pure cobalt pyridine amidates detection of soluble assemblies with stoichiometry corresponding to the solid state, *Dalton. Trans*., 2011, **40**, 1722–1731; (*b*) T. Paunesku, S. Vogt, J. Maser, B. Lai and G. Woloschak, X-ray fluorescence microprobe imaging in biology and medicine, *J. Cell. Biochem*., 2006, **99**, 1489–1502; (*c*) Z. Qin, J. A. Caruso, B. Lai, A. Matusch and J. S. Becker, Trace metal imaging with high spatial resolution: applications in biomedicine, *Metallomics*, 2011, **3**, 28–37.

3 (*a*) I. Bertini, H. B. Gray, E. I. Stiefel, J. S. Valentine,, University Science Books, Sausalito, CA, 2007, p. 739; (*b*) S. J. Lippard and J. M. Berg, *Principles of Bioinorganic Chemistry*, University Science Books, Mill Valley, CA, 1994.

4 K. Richter, M. Schicklberger and J. Gescher, Dissimilatory reduction of extracellular electron acceptors in anaerobic respiration, *Appl. Environ. Microbiol*., 2012, **78**, 913–921.

5 J. K. Fredrickson, M. F. Romine, A. S. Beliaev, J. M. Auchtung, M. E. Driscoll, T. S. Gardner, K. H. Nealson, A. L. Osterman, G. Pinchuk, J. L. Reed, D. A. Rodionov, J. L. Rodrigues, D. A. Saffarini, M. H. Serres, A. M. Spormann, I. B. Zhulin and J. M. Tiedje, Towards environmental systems biology of *Shewanella*, *Nat. Rev. Microbiol*., 2008, **6**, 592–603.

6 J. F. Heidelberg, I. T. Paulsen, K. E. Nelson, E. J. Gaidos, W. C. Nelson, T. D. Read, J. A. Eisen, R. Seshadri, N. Ward, B. Methe, R. A. Clayton, T. Meyer, A. Tsapin, J. Scott, M. Beanan, L. Brinkac, S. Daugherty, R. T. DeBoy, R. J. Dodson, A. S. Durkin, D. H. Haft, J. F. Kolonay, R. Madupu, J. D. Peterson, L. A. Umayam, O. White, A. M. Wolf, J. Vamathevan, J. Weidman, M. Impraim, K. Lee, K. Berry, C. Lee, J. Mueller, H. Khouri, J. Gill, T. R. Utterback, L. A. McDonald, T. V. Feldblyum, H. O. Smith, J. C. Venter, K. H. Nealson and C. M. Fraser, Genome sequence of the dissimilatory metal ion-reducing bacterium *Shewanella oneidensis*, *Nat. Biotechnol*., 2002, **20**, 1118–1123.

7 (*a*) A. S. Beliaev, D. K. Thompson, T. Khare, H. Lim, C. C. Brandt, G. Li, A. E. Murray, J. F. Heidelberg, C. S. Giometti, J. Yates, 3rd, K. H. Nealson, J. M. Tiedje and J. Zhoui, Gene and protein expression profiles of *Shewanella oneidensis* during anaerobic growth with different electron acceptors, *OMICS*, 2002, **6**, 39–60; (*b*) M. D. Blakeney, T. Moulaei and T. J. DiChristina, Fe(III) reduction activity and cytochrome content of *Shewanella putrefaciens* grown on ten compounds as sole terminal electron acceptor, *Microbiol. Res*., 2000, **155**, 87–94.

8 T. E. Kehl-Fie and E. P. Skaar, Nutritional immunity beyond iron: a role for manganese and zinc, *Curr. Opin. Chem. Biol*., 2010, **14**, 218–224.

9 M. González-Guerrero, D. Raimunda, X. Cheng and J. M. Argüello, Distinct functional roles of homologous Cu^+ efflux ATPases in *Pseudomonas aeruginosa*, *Mol. Microbiol*., 2010, **78**, 1246–1258.

10 J. Szpunar, Advances in analytical methodology for bioinorganic speciation analysis: metallomics, metalloproteomics and heteroatom-tagged proteomics and metabolomics, *Analyst*, 2005, **130**, 442–465.

11 (*a*) S. Tottey, C. J. Patterson, L. Banci, I. Bertini, I. C. Felli, A. Pavelkova, S. J. Dainty, R. Pernil, K. J. Waldron, A. W. Foster and N. J. Robinson, Cyanobacterial metallochaperone inhibits deleterious side reactions of copper, *Proc. Natl. Acad. Sci. U. S. A*., 2012, **109**, 95–100; (*b*) M. Gonzalez-Fernandez, T. Garcia-Barrera and J. L. Gomez-Ariza, Molecular mass spectrometric identification of superoxide dismutase in the liver of mice Mus musculus and Mus spretus using a metallomics analytical approach, *Anal. Bioanal. Chem*., 2011, **401**, 2779–2783.

12 J. S. Becker, D. Pozebon, A. Matusch, V. L. Dressler and J. S. Becker, Detection of Zn-containing proteins in slug (Genus Arion) tissue using laser ablation ICP-MS after separation by gel electrophoresis, *Int. J. Mass Spectrom*., 2011, **307**, 66–69.

13 A. M. Sevcenco, M. W. Pinkse, H. T. Wolterbeek, P. D. Verhaert, W. R. Hagen and P. L. Hagedoorn, Exploring the microbial metalloproteome using MIRAGE, *Metallomics*, 2011, **3**, 1324–1330.

14 (*a*) Y. Dong, Y. X. Gao, C. Y. Chen, B. Li, X. Li, H. W. Yu, W. He, Y. Y. Huang and Z. F. Chai, Quantification of trace elements in protein bands using synchrotron radiation X-ray fluorescence after electrophoretic separation, *Chin. J. Anal. Chem*., 2006, **34**, 443–446; (*b*) Y. X. Gao, Y. B. Liu, C. Y. Chen, B. Li, W. He, Y. Y. Huang and Z. F. Chai, Combination of synchrotron radiation X-ray fluorescence with isoelectric focusing for study of metalloprotein distribution in cytosol of hepatocellular carcinoma and surrounding normal tissues, *J. Anal. At. Spectrom*., 2005, **20**, 473–475; (*c*) M. Kuhbacher, G. Weseloh, A. Thomzig, H. Bertelsmann, G. Falkenberg, M. Radtke, H. Riesemeier, A. Kyriakopoulos, M. Beekes and D. Behne, Analysis and localization of metal- and metalloid-containing proteins by synchrotron radiation X-ray fluorescence spectrometry, *X-Ray Spectrom*., 2005, **34**, 112–117; (*d*) G. Weseloh, M. Kuhbacher, H. Bertelsmann, M. Ozaslan, A. Kyriakopoulos, A. Knochel and D. Behnel, Analysis of metal-containing proteins by gel electrophoresis and synchrotron radiation X-ray fluorescence, *J. Radioanal. Nucl. Chem*., 2004, **259**, 473–477; (*e*) F. M. Verbi, S. C. Arruda, A. P. Rodriguez, C. A. Perez and M. A. Arruda, Metal-binding proteins scanning and determination by combining gel electrophoresis, synchrotron radiation X-ray fluorescence and atomic spectrometry, *J. Biochem. Biophys. Methods*, 2005, **62**, 97–109; (*f*) S. Chevreux, S. Roudeau, A. Fraysse, A. Carmona, G. Deves, P. L. Solari, S. Mounicou, R. Lobinski and R. Ortega, Multimodal analysis of metals in copper-zinc superoxide dismutase isoforms separated on electrophoresis gels, *Biochimie*, 2009, **91**, 1324–1327; (*g*) A. Sussulini, J. S. Garcia, M. F. Mesko, D. P. Moraes, E. M. M. Flores, C. A. Perez and M. A. Z. Arruda, Evaluation of soybean seed protein extraction focusing on metalloprotein analysis, *Microchim. Acta*, 2007, **158**, 173–180.

15 L. Finney, Y. Chishti, T. Khare, C. Giometti, A. Levina, P. A. Lay and S. Vogt, Imaging metals in proteins by combining electrophoresis with rapid X-ray fluorescence mapping, *ACS Chem. Biol*., 2010, **5**, 577–587.

16 B. S. Twining, S. B. Baines, N. S. Fisher, J. Maser, S. Vogt, C. Jacobsen, A. Tovar-Sanchez and S. A. Sanudo-Wilhelmy, Quantifying trace elements in individual aquatic protist cells with a synchrotron X-ray fluorescence microprobe, *Anal. Chem*., 2003, **75**, 3806–3816.
17 M. A. Jacobs, A. Alwood, I. Thaipisuttikul, D. Spencer, E. Haugen, S. Ernst, O. Will, R. Kaul, C. Raymond, R. Levy, L. Chun-Rong, D. Guenthner, D. Bovee, M. V. Olson and C. Manoil, Comprehensive transposon mutant library of *Pseudomonas aeruginosa*, *Proc. Natl. Acad. Sci. U. S. A*., 2003, **100**, 14339–14344.
18 O. H. Lowry, N. J. Rosebrough, A. L. Farr and R. J. Randall, Protein measurement with the Folin phenol reagent, *J. Biol. Chem*., 1951, **193**, 265–275.
19 U. K. Laemmli, Cleavage of structural proteins during the assembly of the head of bacteriophage T4, *Nature*, 1970, **227**, 680–685.
20 S. Vogt, MAPS: A set of software tools for analysis and visualization of 3D X-ray fluorescence data sets, *J. Phys. IV France*, 2003, **104**, 635–638.
21 C. S. Giometti, T. Khare, S. L. Tollaksen, A. Tsapin, W. H. Zhu, J. R. Yates and K. H. Nealson, Analysis of the *Shewanella oneidensis* proteome by two-dimensional gel electrophoresis under nondenaturing conditions, *Proteomics*, 2003, **3**, 777–785.
22 M. E. Marquart, A. R. Caballero, M. Chomnawang, B. A. Thibodeaux, S. S. Twining and R. J. O'Callaghan, Identification of a novel secreted protease from *Pseudomonas aeruginosa* that causes corneal erosions, *Invest. Ophthalmol. Visual Sci*., 2005, **46**, 3761–3768.
23 H. Katoh, N. Hagino, A. R. Grossman and T. Ogawa, Genes essential to iron transport in the cyanobacterium *Synechocystis* sp. strain PCC 6803, *J. Bacteriol*., 2001, **183**, 2779–2784.
24 N. Koropatkin, A. M. Randich, M. Bhattacharyya-Pakrasi, H. B. Pakrasi and T. J. Smith, The structure of the iron-binding protein, FutA1, from *Synechocystis* 6803, *J. Biol. Chem*., 2007, **282**, 27468–27477.
25 A. Badarau, S. J. Firbank, K. J. Waldron, S. Yanagisawa, N. J. Robinson, M. J. Banfield and C. Dennison, FutA2 is a ferric binding protein from *Synechocystis* PCC 6803, *J. Biol. Chem*., 2008, **283**, 12520–12527.
26 C. V. Rosadini, J. D. Gawronski, D. Raimunda, J. M. Argüello and B. J. Akerley, A novel zinc binding system, ZevAB, is critical for survival of nontypeable *Haemophilus influenzae* in a murine lung infection model, *Infect. Immun*., 2011, **79**, 3366–3376.
27 (*a*) P. A. Clohessy and B. E. Golden, Calprotectin-mediated zinc chelation as abiostatic mechanism in host defence, *Scand. J. Immunol*., 1995, **42**, 551–556; (*b*) D. Legrand, E. Elass, M. Carpentier and J. Mazurier, Lactoferrin: a modulator of immune and inflammatory responses, *Cell. Mol. Life Sci*., 2005, **62**, 2549–2559.
28 B. D. Corbin, E. H. Seeley, A. Raab, J. Feldmann, M. R. Miller, V. J. Torres, K. L. Anderson, B. M. Dattilo, P. M. Dunman, R. Gerads, R. M. Caprioli, W. Nacken, W. J. Chazin and E. P. Skaar, Metal chelation and inhibition of bacterial growth in tissue abscesses, *Science*, 2008, **319**, 962–965.
29 T. Khare, Y. Chishti and L. Finney, in *Protein Electrophoresis and Detection: Methods and Protocols*, ed. B. T. Kurien and R. H. Scofield, Humana Press/Springer Science, New York, New York, 2012.
30 A. M. Sevcenco, G. C. Krijger, M. W. Pinkse, P. D. Verhaert, W. R. Hagen and P. L. Hagedoorn, Development of a generic approach to native metalloproteomics: application to the quantitative identification of soluble copper proteins in *Escherichia coli*, *J. Biol. Inorg. Chem*., 2009, **14**, 631–640.
31 A. Cvetkovic, A. L. Menon, M. P. Thorgersen, J. W. Scott, F. L. Poole 2nd, F. E. Jenney, Jr., W. A. Lancaster, J. L. Praissman, S. Shanmukh, B. J. Vaccaro, S. A. Trauger, E. Kalisiak, J. V. Apon, G. Siuzdak, S. M. Yannone, J. A. Tainer and M. W. Adams, Microbial metalloproteomes are largely uncharacterized, *Nature*, 2010, **466**, 779–782.
32 S. Tottey, K. J. Waldron, S. J. Firbank, B. Reale, C. Bessant, K. Sato, T. R. Cheek, J. Gray, M. J. Banfield, C. Dennison and N. J. Robinson, Protein-folding location can regulate manganese-binding *versus* copper- or zinc-binding, *Nature*, 2008, **455**, 1138–1142.